Transactions of the Materials Research Society of Japan 26 [2] 573-576 (2001)

Sol – Gel Transition and Gel Structure of Rod – Shaped Protein

Rio Kita, Makoto Kaibara and Kenji Kubota*
The Institute of Physical and Chemical Research (RIKEN), Wako, Saitama 351-0198, Japan
Fax: 81-48-467-9389, e-mail: rkita@postman.riken.go.jp
*Faculty of Engineering, Gunma University, Kiryu, Gunma 376-8518, Japan
Fax: 81-277-30-1447, e-mail: kkubota@bce.gunma-u.ac.jp

Fibrinogen is a rod shaped protein with the molecular weight of 34×10^4, and shows a unique sol-gel transition behavior. Dynamic process of the formation of fibrin gel was investigated by dynamic light scattering. Temporal evolution of the characteristic decay time distribution confirmed the stepwise gelation mechanism. The gel structure was analyzed by correlation functions of scattering light intensity. At the gelation point, the correlation function showed a power law behavior, and the fractal dimension of the network structure was about 1.4 which was deduced from the exponent of its power law behavior.
Key words: Fibrinogen, Sol-gel transition, Dynamic light scattering

1. INTRODUCTION

Fibrinogen is the structural protein, which forms fibrin blood clots, and plays an essential role in various pathological processes. The transformation of fibrinogen into fibrin gel is thought to involve a series of aggregation steps. The conversion from fibrinogen to fibrin is initiated by the specific cleavage by the serine protease, thrombin. The binding sites at central domain of fibrin interact with complementary sites on the end groups of two other fibrin molecules. The spontaneous association of fibrin monomers forms oligomers with staggered overlapping of chains. The resultant stranded protofibrils further aggregate laterally in the succeeding step to form fibers, and a three-dimensional network, which is responsible for the characteristic clotting or the fibrin gel, results in the further growth of network [1]. Dynamic process of the respective step from fibrinogen to fibrin gel has been studied from the rheological aspects [2,3] and light scattering and turbidity methods [4,5,6,22]. The structural information of the protofibrils and fibers has also been investigated by electron microscopy [7,8,9]. In order to clarify the gelling process, kinetic analyses were carried out extensively [9,10]. However, it is difficult to characterize the physicochemical properties of fibrin and/or protofibrils in the respective step during the time course of gelation, because the system is in the reaction process. From these viewpoints, we attempted to study the time evolution of dynamic light scattering to elucidate the dynamic process from fibrinogen to protofibril, the lateral aggregation of protofibril, and the formation of gel network by analyzing the temporal evolution of dynamic light scattering. The structure of fibrin gel network was also investigated.

2. EXPERIMENTAL

Bovine fibrinogen (clottability 97%) was obtained from Sigma-Aldrich Co., and was dissolved in a phosphate buffer solution with pH 7.4, which consists of Na_2HPO_4, KH_2PO_4, KCl, and NaCl. Concentration of the fibrinogen solution was adjusted to 0.22 g/100 ml. Purified bovine thrombin obtained from Mochida Co., Japan was also dissolved in the phosphate buffer solution at the concentration of 10 NIH units/ml. Before mixing the fibrinogen and thrombin solutions, both of the sample solutions were incubated at 37°C for 15 minutes. Just before the measurements, the solutions of fibrinogen and thrombin were mixed at a volume ratio of 500:1, and this time of mixing was denoted as elapsed time t = 0 in the time course of gelation process. A low concentration of thrombin was used to ensure the measurement of the time evolution. For the light scattering measurement, the mixed solution was immediately put into a cylindrical cell with an optical path length of 6mm by passing it through a membrane filter of 0.2 μm pore size. The preparation was carried out in a clean dry box in order to prevent contamination of impurities.

Dynamic light scattering measurement was carried out using a homemade spectrometer and an ALV-5000 multiple-tau digital correlator to obtain the correlation function of scattered light $g^{(2)}(\tau)$ and the averaged scattered light intensity $< I >$ simultaneously. The decay time distribution function $G(\tau^*)$ was obtained from $g^{(2)}(\tau)$ using CONTIN program. Light source was a He-Ne laser with the wavelength λ = 632.8 nm and the details of apparatus was described elsewhere [11]. The measurements of $g^{(2)}(\tau)$ in the time course of gelation were carried out at 37 °C and at the scattering angle θ = 30°, and were obtained by the homodyne mode.

3. DATA ANALYSIS

The correlation functions of scattered light intensity $g^{(2)}(\tau)$ were analyzed by the inverse Laplace transformation program (constrained regularization program, CONTIN). The $g^{(2)}(\tau)$ has the following form related to the normalized electric field correlation function, $g^{(1)}(\tau)$ as

$$g^{(2)}(\tau) - 1 = b|g^{(1)}(\tau)|^2 \quad (1)$$

where b is a machine constant relating to the coherence of detection. Generally, $g^{(1)}(\tau)$ is expressed by the distribution function $G(\tau^*)$ as a function of the characteristic decay time τ^* as

$$g^{(1)}(\tau) = \int G(\tau^*) \exp(-\tau / \tau^*)\, d\tau^* \quad (2)$$

where $\int G(\tau^*)\, d\tau^* = 1$. That is, $g^{(1)}(\tau)$ is the Laplace transform of $G(\tau^*)$.

At the gelation point, three dimensional network structure develops upto the macroscopic scale and the density (concentration) fluctuation becomes to have a self-similar nature. Therefore, the correlation function $g^{(1)}(\tau)$ does not have the characteristic time and shows a power law behavior as has been observed in various gelling systems [12,13],

$$g^{(1)}(\tau) \sim \tau^{-\phi}, \quad (3)$$

then, $g^{(2)}(\tau)$ is expressed as a sum of a cooperative diffusional mode relating to the entangled (crossbridged) structure and a power law behavior, which was reported first by Martin et al. [14] as

$$g^{(2)}(\tau)-1 = [A \exp(-\tau/\tau_f) + (1-A)(1 + \tau/\tau')^{-\phi}]^2. \quad (4)$$

Here A is an amplitude factor of the relative scattered intensity, and τ_f and τ' are the characteristic decay time of the fast (cooperative) mode and the lower cutoff time of the power law behavior, respectively. The exponent ϕ relates to the fractal dimension. On the other hand, $g^{(2)}(\tau)$ of the pregel solution is well described by the stretched exponential form as

$$g^{(2)}(\tau)-1 = \{A \exp(-\tau/\tau_f) + (1-A) \exp[-(\tau/\tau_s)^{\beta}]\}^2. \quad (5)$$

Here τ_s is the characteristic decay time of the slow mode. Approaching the sol-gel transition point, correlation function $g^{(2)}(\tau)$ changes from the stretched exponential form to the power-law one with β decreasing to zero and τ_s diverging [14].

In consideration of the gelation of polymer system, the mass fractal of the developed cluster is expressed with the molecular weight M and its characteristic size R as $M \sim R^{Df}$, where D_f is the fractal dimension [15]. Such a scaling behavior has been discussed extensively in terms of the percolation model [16,17]. The electric field correlation function $g^{(1)}(\tau)$ is the time correlation function associated to the density fluctuation, $<\rho_k(0)\rho_{-k}(t)>$. Here $\rho_k(t)$ denotes the magnitude of concentration fluctuation having the wavelength of k at time t. Generally, the density–density correlation function of a fractal is expressed as the power law $<\rho(0)\rho(r)> \sim r^{-(d-Dp)}$ [15]. In this analogy, $g^{(1)}(\tau)$ could be shown as the fractal with the dimension of time being d=1, and the fractal time set of detected photons is given as

$$g^{(2)}(\tau) - 1 \sim \tau^{-2(1-Dp)} \quad (6)$$

where D_p is a fractal dimension of scattered photons and is related to the structure of gelling cluster in the percolation theory for sol-gel transition [14,16]. The value of D_p is sensitive to the degree of branching in a gel and correlates to a topological and structural nature of gel. At the gelation point, we obtain the relation from Eqs. 4 and 6 as,

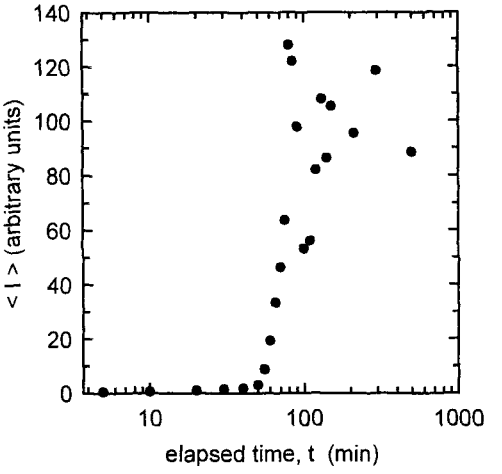

Fig. 1. Time evolution of the scattered light intensity at $\theta = 30^\circ$ for the fibrinogen-thrombin system.

$$\phi = 1 - D_p. \quad (7)$$

In a typical rheological measurement at the gelation point, the storage modulus G' and loss modulus G'' behave as a power law against the function of frequency [20],

$$G'(\omega) \sim G''(\omega) \sim \omega^n. \quad (8)$$

The physical meaning of the exponent n and D_p is equivalent, since the dynamical structure factor $g^{(1)}(\tau)$ corresponds to the (imaginary part of) complex dynamical longitudinal compliance [17]. The relationship between the exponent n and the fractal dimension D_f has been derived by Muthukumar [21] and Martin et al. [14] with taking into account the screening of excluded volume effect as

$$n = d/(D_f + 2) \quad (9a)$$

$$= d/(D_f' + 2) = d(d+2-2D_f)/2(d+2-D_f) \quad (9b)$$

where (9a) and (9b) correspond to the case with (unscreening) and without (screening) the excluded volume effect, respectively. The magnitude of n is significantly affected by the excluded volume effect.

4. RESULTS AND DISCUSSION

Figure 1 shows the scattered light intensity $< I >$ as a function of the elapsed time t. The scattered light intensity showed a very low value for $t < 50$ min. However, the intensity increased rapidly and enormously at $50 < t < 80$ min, and then showed a leveling-off tendency. These behaviors can be separated into three steps: namely, (1) initial lag and/or slow increase, (2) rapid increase, and (3) saturation behavior of intensity. It is noteworthy that the scattered light intensity showed oscillating and nonergodic behavior at the third step. Since the scattered light intensity corresponds to the molecular weight of independently dispersing particles, the increase of scattered light intensity is related to the growth of aggregating clusters until the gelation point. Overall behavior of the scattered light intensity against the elapsed time is similar to the previous works of fibrinogen solutions studied by light scattering [4] and

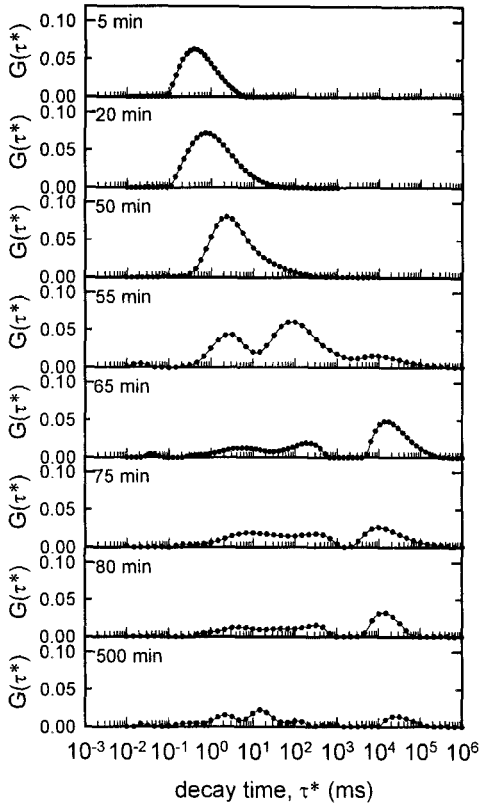

Fig. 2. Typical result of time evolution of the decay time distribution function G(τ*).

turbidity [9].

Figure 2 shows the time evolution of the decay time distribution function G(τ*). The G(τ*) of polymer solution reflects the molecular weight distribution of polymer and/or oligomer. Rigorously speaking, this is true only in a dilute limit, since there exists an effect of concentration dependence. However, in the present case the concentration of fibrinogen is quite low, and such a treatment can be applied upto the sol-gel transition point as mentioned above. At t = 5 min, G(τ*) showed a unimodal distribution in the short decay time region. G(τ*) of fibrinogen solution without thrombin is almost the same as that at t = 5 min, except for having a narrower distribution. With increasing the elapsed time, the distribution becomes broader and shifts to longer decay time. The behavior of G(τ*) at t < 50 min (corresponding to the first stage of <I> vs t in Fig.1) indicates that the molecular weight of fibrin oligomers became larger and formation of protofibrils proceeds. Effect of thrombin itself to G(τ*) can be neglected, because of the very low concentration of thrombin compared to fibrinogen and its low molecular weight. The distribution function changes its shape dramatically and qualitatively with the appearance of two other modes in the slower decay time region for t ≧ 55 min. At t = 55 min the middle peak has larger intensity than the slowest one. The G(τ*) at t = 50 min shows a slight shoulder in the tail region at $\tau^* = 10^1 \sim 10^2$ ms, and it corresponds to the middle peak of G(τ*) at t = 55 min. The fluctuation mode corresponding to such time region results from the fiber formation of protofibrils by the lateral aggregation of them. This picture is consistent

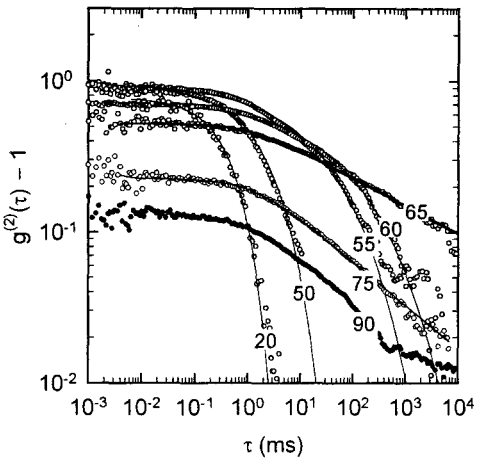

Fig. 3. Double-logarithmic plots of correlation function $g^{(2)}(\tau) - 1$ as a function of delay time τ. Numbers in the figure mean elapsed time, t (min). Solid curves were calculated by stretched exponential (Eq. 5) for t ≦ 60 min and power law (Eq. 4) for t ≧ 65 min.

with the rapid increase of scattered light intensity (2nd step). At t = 65 min, the intensity of the middle and fastest modes decrease, but that of the slowest one increases very much. With the further increase of elapsed time, the intensity of the slowest mode again decreases relative to the middle and fastest modes (t =75 and 80 min).

After the formation of protofibril was fulfilled enough (~ 50 min), the lateral aggregation of protofibrils occurs (55 min) and the formation of gel cluster follows (55 ~ 65 min). The slowest relaxation mode should relates to the fibrin gel clusters showing the very slow decay rate ($\tau^* = 10^4 \sim 10^5$ ms), and remains even in the subsequent elapsed time for t > 65 min. The decrease of intensity of the slowest mode of G(τ*) with increasing elapsed time at t > 65 min is due to the decrease of contrast in density profile by the further growth of network. However, such growth of network structure by the lateral aggregation results finally in the freezing of fluctuation and local network structure (appearance of nonergodicity), and the correlation function becomes to exhibit a long time tail, after about t = 90 min (beginning of the 3rd step of <I> vs t in Fig. 1). In this time range, a remarkable decrease of coherence factor b of Eq. (1) is observed in agreement with the frozen inhomogeneity. At t = 500 min, the fastest mode became faster again. This fastest mode results from the cooperative diffusional motion of the network structure as observed for entangled and/or gelling polymer solutions. Because of the stiff nature of fibrin fibers, density fluctuation due to the cooperative diffusion of gel network is rather weak compared to the case of flexible polymer solutions.

The lateral aggregation between protofibrils (t > 50 min) results in the network formation and gelation. The longest relaxation mode appears at $\tau^* = 10^4 - 10^5$ ms at the elapsed time t = 55 min, and this mode grows up the most largest mode at t = 65 min. These behaviors clarified that the conversion of fibrinogen to protofibrils and the gelation proceed in a stepwise manner.

Figure 3 shows double-logarithmic plots of

correlation function $g^{(2)}(\tau)$ - 1 as a function of delay time τ. The $g^{(2)}(\tau)$ - 1 shows a characteristic decay behavior similar to the usual polymer solution with very broad decay time distribution for $t \leqq 60$min. However for $t \geqq 90$ min, $g^{(2)}(\tau)$ - 1 becomes to show a long time tail in the range of long delay time. In fact, a least squares fit to the stretched exponential formula (Eq. 5) shows a good agreement for $t \leqq 60$ min, but shows systematic deviations for $t \geqq 65$ min. On the other hand, the power law relation (Eq. 4) can be fitted well to the experimental data points for $t = 65$ min. The existence of the characteristic delay time of slow mode, τ_s, means that the relaxation time of cluster is finite, i.e., the system is in the sol state. With increasing the elapsed time until $t = 60$ min, the decay time of the slow mode τ_s increases from 1.03 to 442 ms. The exponent β of stretched exponential relation decreases from 0.87 to 0.33. These tendencies are reasonable for the sol state, because β should decrease to 0 and τ_s should diverge at the gelation point.

The validity of power law around at $t = 65$ min means that the decay behavior is independent of the time scale, i.e., the clusters which are composed of fibrin fibers become to have a self-similar structure in the large scale compared with the molecular size of fibrinogen. Since sol-gel transition point is defined as that at least one of the clusters of the crosslinking polymer grows and reaches the macroscopic size, the elapsed time of $t = 65$ min can be notified as the formation of fibrin gel and the gelation point, and this is consistent with the results of the decay time distribution of Fig. 2.

At the sol to gel transition point ($t = 65$ min), we obtained the exponent of power law behavior as $\phi = 0.093 \pm 0.004$. The fractal dimension of the scattered photons is calculated from Eq. 7 as D_p=0.91 and the fractal dimension evaluated as $D_f = 1.42$ from Eq. 9a. In the present case that rigid fibrin fibers form fibrin gel network, then the excluded volume effect should not contribute. Percolation theory predicts $D_f = 5/2$, which is substantially larger than the present value. Generally, D_p (or n) for the gel constructed by flexible polymers are reported to be within 1/2 to 2/3, but these values are known to depend strongly on the cross-linking density of network and network structure. For linear polymer systems with screening of the excluded-volume effect, D_p is shown to be 1/2, and for polydisperse polymer systems is shown to be 2/3 according to the percolation theory. In fact, Shibayama and co-workers reported for silica gel using the dynamic light scattering [19], and showed that D_p increases with increasing degree of branching. Winter et al. reported by the rheological measurements that the frequency dependence as described in Eq. 8 gave $0.5 < n < 0.7$ for a polyurethanes system [20]. From the theoretical aspect, Muthukumar discussed the relation of n with the fractal dimension considering the excluded-volume effect [21]. These results indicate that the fractal dimension of the gelling system is not universal, but depends on the stoichiometry and network structure (excluded volume).

The fractal dimension D_f=1.42 evaluated for fibrinogen-thrombin system is rather close to the value for the case of deficiency of crosslinking and the structure of gel is inhomogeneous: that is, crosslinking does not occur homogeneously in the medium, but occurs locally with substantial spatial variation. Moreover, a small value of fractal dimension means that network is loose and anisotropic one. Branching occurs concentratedly at respective crosslinking point (or region), but the number density of crosslinking should be low. These should be due to the fact that network consists of rigid fibrin fibers (lateral aggregates of protofibrils). Such a loose structure will result in high permeability of solvent through the fibrin gel and low osmotic pressure effect of the fibrin gel.

Investigation of the macroscopic nature of fibrin gel in a test tube gives another characteristics of the fibrin gel. At $t = 24$ hours later, the gel in the tube shows syneresis by its own gravity effect, although such a behavior depends on the concentration of fibrinogen and thrombin. It means that the fibrin gel in this experimental condition is very weak in terms of macroscopic rigidity: that is, the binding strength of the gel might be very weak because of the sparse gel network.

REFERENCES

[1] J. W. Weisel, *Biophys. J.*, **50**, 1079-1093 (1986).
[2] M. Kaibara, *Polym. Gels Networks*, **2**, 1-28 (1994).
[3] A. E. Ryan, F. L. Mockros, W. J. Weisel, and L. Lorand, *Biophys. J.*, **77**, 2813-2826 (1999).
[4] R, R. Hantgan and J. Hermans. *J. Biol. Chem.*, **254**, 11272-11281 (1979).
[5] M. E. Carr and J. Hermans, *Macromolecules* **11**, 52-56 (1978).
[6] S. Bernocco, F. Ferri, A. Profumo, C. Cuniberti and M. Rocco, *Biophys. J.*, **79**, 561-583 (2000).
[7] L. Medved', T. Ugarova, Y. Veklich, N. Lukinova. and J. Weisel, *J. Mol. Biol.*, **216**, 503-509 (1990).
[8] Y. Veklich, C. W. Francis, J. White. and J. W. Weisel. *Blood*, **92**, 4721-4729 (1998).
[9] J. W. Weisel and C. Nagaswami, *Biophys. J.*, **63**, 111-128 (1992).
[10] M. Kaibara, *Biorheology*, **10**, 61-73 (1973).
[11] K. Kubota, H. Urabe, Y. Tominaga., and S. Fujime. *Macromolecules*, **17**, 2096-2104 (1984).
[12] A. Onuki, *J. Non-Cryst. Solids*, **172-174**, 1151-1157 (1994).
[13] M. Tsianou, A. –L. Kjoniksen, K. Thuresson and B. Nystrom, *Macromolecules*, 32, 2974-2982 (1999).
[14] J. E. Martin., and J. P. Wilcoxon, *Phys. Rev. Lett.*, **61**, 373-376 (1988).
[15] B. B. Mandelbrot, "The fractal geometry of nature", Freeman, San Francisco (1982).
[16] D. Stauffer, A. Coniglio and M. Adam, *Adv. Poly. Sci.*, **44**, 103-158 (1982).
[17] M. Adam and D. Lairez, "The Physical Properties of Polymer Gels", Ed. By J. P. Cohen Addad, Jhon Wiley & Sons Ltd, NY (1996).
[18] D. L. Tipton and P. S. Russo, *Macromolecules*, **29**, 7402-7411 (1996).
[19] T. Norisuye, M. Inoue, M. Shibayama, R. Tamaki and Y. Chujo, *Macromolecules*, **33**, 900-905 (2000).
[20] H. H. Winter, P. Morganelli and F. Chambon, Macromolecules **21**, 532-582 (1988).
[21] M. Muthukumar, *Macromolecules*, **22**, 4656-4658 (1989).
[22] P. Wiltzius, G. Dietler, W. Kanzig, A. Haberli, and P. W. Straub, *Biopolymers*, **21**, 2205-2223 (1982).

(Received December 8, 2000; Accepted February 16, 2001)